Data, Innovation, and Science Cluster

Swarm Ion Temperature Estimate: Validaton Report

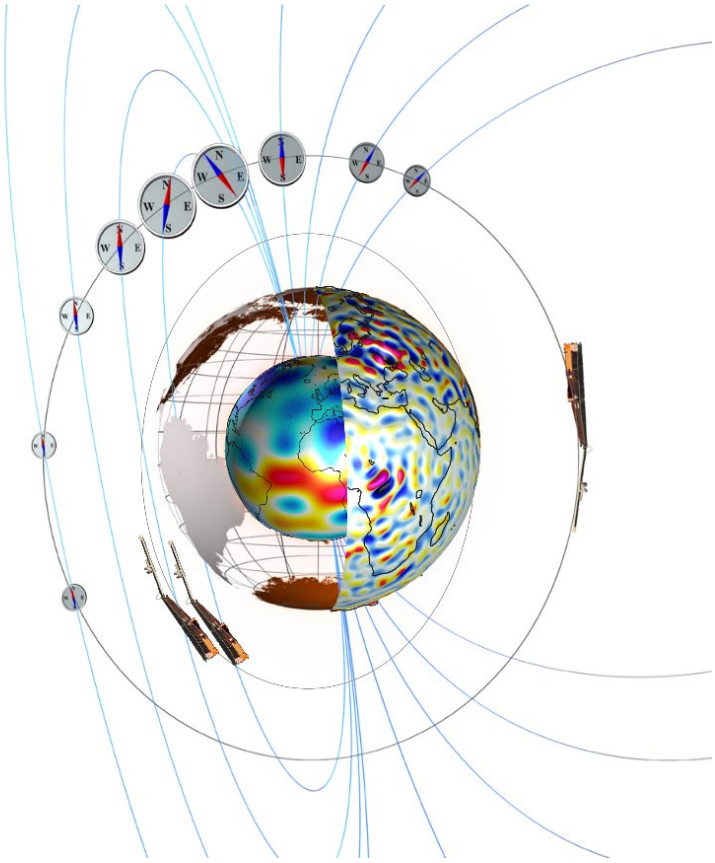

Doc. no: SW-TN-UoC-GS-005: 1, 17 Jan 2022

Prepared:

Levan Lomidze — Date 17 Jan 2022

Project Scientist

Approved:

Johnathan Burchill — Date 17 Jan 2022

Project Manager

Record of Changes

Reason	Description	Rev	Date
Initial vers.	Draft	1dA	12 FEB 2021
Release	Signed and released	1	17 Jan 2022

Table of Contents

Table of Figures

1 Introduction

This document reports on the validation results of Swarm Ion Temperature Estimation (SITE) data products. It focuses on the calibration and validation of the primary inputs of the ion temperature model: Swarm Langmuir probe (LP) electron densities (Ne) and electron temperatures (Te) (between Dec/2013-Jul/2020), Swarm Thermal Ion Imagers (TII) high-latitude cross-track, along-track, and vertical ion drifts (between Dec/2013-Sept/2020), and on the preliminary validation of the estimated ion temperatures (Ti) in the top-side ionosphere (between Dec/2013-May/2017) for each Swarm satellite.

The LP Ne, Te and SITE Ti data were compared to corresponding coincident measurements from six different Incoherent scatter radars (ISRs) located at low, middle, and high geomagnetic latitudes in the northern hemisphere. The comparison for Te was performed separately for high-gain and low-gain LP data. The initial (uncorrected) Swarm LP data shows that electron densities are systematically low by ~20 % and electron temperatures are systematically high by about 13 % and 30 % for high-gain and low-gain LP, respectively. The LP data were recalibrated using the ISR data to remove systematic errors prior to using them for the Ti estimation. The new calibration results are in agreement with their previously reported calibration and validation results for Ne and high-gain Te. The low-gain LP Te data show larger deviations from their independent measurements. The corrected Swarm LP data are well suited for SITE.

The validation of TII high-latitude ion drift data (ver 0302) was conducted by examining the variation of median ion drifts by magnetic latitude (MLAT), magnetic local time (MLT), and interplanetary magnetic field (IMF) orientation in northern and southern hemisphere. In addition, the MLAT-MLT distributions of the ion drifts were compared to the corresponding estimates from the Weimer 2005 empirical convection electric field model. The new version of the TII data used in the validation report shows improved cross-track estimates, which are in good agreement with the empirical model. Even though some promising results are obtained for the along-track and vertical drifts, it is suggested that their current estimates to be omitted from the SITE.

The comparison of SITE Ti data to the ISR measurements reveals that the Ti estimates are sufficiently close to their independent measurements (within ~ 14 % or 140 K (1-sigma)) and exhibit strong correlation (0.63-0.84), which changes depending on the satellite and its LP measurement mode. The local time and latitude variations also agree with the expected picture. It was found that the SITE ion temperature data show systematic errors (overestimation) by ~ 12 % across all Swarm satellites when compared to Incoherent scatter radars. At high latitudes the two separate estimates of the ion temperature, which are based on Swarm TII and Weimer 2005 drifts, differ in magnitude the latter being typically smaller. Currently present issues in SITE data are noted and their possible solutions are briefly discussed.

1.1 Scope and applicability

This document is a deliverable of the Swarm Ion Temperature Estimation project [AD-1].

2 Applicable and Reference Documentation

2.1 Applicable Documents

The following documents are applicable to the definitions within this document.

[AD-1] SW-CO-DTU-GS-123, Rev: 1A 2019-10-08, Subcontract SITE 2.3.

2.2 Abbreviations

A list of acronyms and abbreviations used by Swarm partners can be found here. Any acronyms or abbreviations not found on the online list but used in this document can be found below.

Acronym ***or abbreviation***	***Description***
NRLMSISE	Naval Research Laboratory Mass Spectrometer and Incoherent Scatter Radar Extended
HWM	Horizontal Wind Model
SITE	Swarm Ion Temperature Estimation

2.3 Reference Documents

The following documents contain supporting and background information to be taken into account during the activities specified within this document.

[RD-1] Lomidze, L., Knudsen, D. J., Burchill, J., Kouznetsov, A., & Buchert, S. C. (2018). Calibration and validation of Swarm plasma densities and electron temperatures using ground-based radars and satellite radio occultation measurements. Radio Science, 53.

[RD-2] SW-RN-IRF-GS-005, Extended Set of Swarm Langmuir Probe Data

[RD-3] Lomidze, L., Burchill, J. K., Knudsen, D. J., Kouznetsov, A., & Weimer, D. R. (2019). Validity study of the Swarm horizontal cross-track ion drift velocities in the high-latitude ionosphere. Earth and Space Science, 6.

[RD-4] SW-TN-UoC-GS-002_2-3_SITE, Swarm Ion Temperature Estimation: Input data and model validation

[RD-5] SW-RN-UoC-GS-004, EFI TII Cross-Track Flow Data Release Notes

[RD-6] Weimer, D. R. (2005). Improved ionospheric electrodynamic models and application to calculating Joule heating rates. Journal of Geophysical Research, 110, A05306.

[RD-7] Yau, A. W. and Andre, M. (1997). Sources of Ion outflow in the high latitude ionosphere, Space Sci. Reviews, 80, 1-25.

[RD-8] Picone, J. M., Hedin, A. E., Drob, D. P., & Aikin, A. C. (2002). NRLMSISE-00 empirical model of the atmos-phere: Statistical comparisons and scientific issues. Journal of Geophysical Research, 107(A12), 1468.

[RD-9] Drob, D. P., et al. (2015), An update to the Horizontal Wind Model (HWM): The quiet time thermosphere, Earth and Space Science, 2, doi:10.1002/2014EA000089.

[RD-10] Salah, J. E. (1993). Interim standard for the ion-neutral atomic oxygen collision frequency. Geophysical Research Letters, 20(15), 1543–1546.

[RD-11] Huba, J.D., G. Joyce, and J.A. Fedder (2000), Sami2 is Another Model of the Ionosphere (SAMI2): A new low-latitude ionosphere model, J. Geophys. Res., 105, 23,035.

[RD-12] SW-TN-UoC-GS-004_2-3_SITE, Swarm Ion Temperature Estimation: Processing algorithm description

3 Data validation

3.1 Swarm LP electron densities and temperatures

The first calibration and validation of Swarm LP data was reported by [RD-1] based on about 2.5 years of data available at that time. Here the calibration and validation are revaluated using data from extended period (~7 years) and expanded latitude coverage for the independent measurements.

The altitude profile data of electron density, electron temperature (and ion temperature) measured by five different ISRs located at equatorial, middle, and high latitudes were obtained from the Madrigal database (http://jro-db.igp.gob.pe/madrigal; http://cedar.openmadrigal.org; http://millstonehill.haystack.mit.edu; http://isr.sri.com/madrigal). These ISR stations are located at Jicamarca (11.95° S, 76.87° W), Arecibo (18.34° N, 66.75° W), Millstone Hill (42.62° N, 71.49° W), Poker Flat (65.13° N, 147.47° W), and Resolute Bay (74.73° N, 94.91° W) (the latter includes two ISRs: RISR-N and RISR-C). In addition, elevation angle of observation, and measurement errors associated with each measurement were obtained. The radar operations are not continuous, however the time period for which each station has an overlap with Swarm operations are: Nov/2013 – Feb/2020 for Jicamarca, Nov/2013-Feb/2019 for Arecibo, Nov/2013-Mar/2020 for Millstone Hill, Nov/2013-Jul/2020 for Poker Flat, Aug/2015-Feb/2020 For RISR-C, and Jan/2014-Jul/2020 for RISR-N. The LP data are from the "Extended Swarm LP data" [RD-2] between Dec/2017 and Sept/2020.

The criteria for selecting the coincident Swarm and ISR measurements at low and middle latitudes are unchanged from RD-1 except it no longer is limited to comparisons with only geomagnetically quiet periods. For the high-latitude ISRs, the latitude, longitude, and local time differences between them and Swarm satellites are all halved to account for the higher spatial and temporal variability of the high latitude ionosphere. The following is a summary of the data selection criteria. The data comparison is limited to the Swarm satellite passes which are within 2.5° magnetic latitude and 7.5° magnetic longitude (1.25° and 3.25° for high-latitude ISRs, respectively) and local time difference between the ISR and Swarm measurements is taken to be less than or equal to 5 minutes (2.5 minutes at high-latitudes). Furthermore, only near-zenith (elevation angle>80°) ISR measurements are considered. To find the ISR data at Swarm altitudes, the ISR-measured altitude profiles of plasma parameters were interpolated at the altitude of the satellite. The Swarm measurements were down-sampled to 2 second time resolution to speed up the computation. During a given conjunction, all available Swarm data were averaged, and the corresponding standard deviation was also calculated. For the cases when there were several ISR profiles for a given Swarm pass, the average value of the ISR parameter was computed. Therefore, one ISR and one Swarm data point were obtained per conjunction. Included with the ISR profiles are their measurement errors. In the comparison, included were only those ISR measurement which had a relative error <15%, and only those Swarm data for which 1-σ <15%. Finally, to exclude outliers, cases outside $3\tilde{\sigma}$ median difference between the Swarm and ISR were rejected (~7-10 % for Ne, 5-9 % for high-gain LP Te, and ~8 % for low-gain LP Te), where $\tilde{\sigma}$ is a scaled median absolute deviation (equivalent for 1-sigma standard deviation). The total number of points, which are satellite and parameter dependent, varies between 241-324 for Ne, 183-236 for high-gain LP Te, and 204-280 for low-gain LP Te, which are significantly larger than in RD-1 where only select periods between Dec/2013-Jun/2016 were analysed. Note that similar to RD-1 the electron densities are converted to plasma frequencies ($\sim\sqrt{N_e}$) to compare the two. For each conjunction the altitude profiles of the ISR data were visually inspected to ensure only physically reasonable results were included in the comparison and not artefacts due to the altitude interpolation or some other obvious data flaws.

Left panels in Figures 1-3 show a scatter plots of initial Swarm data and their coincident ISR measurements. They correspond to plasma frequency (Figure 1), high-gain Te (Figure 2), and low-gain Te (Figure 3). The data for different ISRs are shown in different colours, and the number of points for a given ISR are also given in the brackets along the legends. Also shown are medians of the absolute and relative differences with their corresponding $\tilde{\sigma}$, and correlation coefficients. Rights panels in Figures 1-3 show how corrected (adjusted/calibrated) Swarm measurements compare to the ISR data. On the left panels are also shown the regression models (with standard errors), which were used to correct the initial Swarm data.

Figure 1 shows that the initial Swarm plasma frequencies are about 10 % lower than the ISR values (equivalently, densities are lower by 21 %), however the correlations are very strong (0.98). The applied correction removes the systematic errors and results in the data which are accurate within about 0.5-0.6 MHz (~20 %). The results are consistent with those previously reported in RD-1, except the new $\tilde{\sigma}$s are larger. Below given are new (and old) regression coefficients with their standard errors, which demonstrate that the changes in the regression models are very small. Note, the earlier version of the Swarm and ISR data comparisons included only low- and middle-latitude ISRs and total number of points were about three times less. In the new comparison there are significant fraction of high latitude measurements (mainly from Poker Flat ISR). The new calibration is applicable for all latitudes, geomagnetic conditions, and density ranges.

Swarm A: $f_{LP}^{adj} = 1.1069(\pm 0.0060) f_{LP}$ (old: $f_{LP}^{adj} = 1.1067(\pm 0.0073) f_{LP}$)

Swarm B: $f_{LP}^{adj} = 1.0952(\pm 0.0071) f_{LP}$ (old: $f_{LP}^{adj} = 1.0882(\pm 0.0089) f_{LP}$)

Swarm C: $f_{LP}^{adj} = 1.1087(\pm 0.0060) f_{LP}$ (old: $f_{LP}^{adj} = 1.1157(\pm 0.0070) f_{LP}$).

Figure 2 compares Swarm high-gain LP Te data to the ISR measurements. It should be noted that in this comparison we ignore the cases where there were LP overflows registered (according to their corresponding) quality flags [RD-2]). The primary reason for this was to avoid sharp drops in the latitudinal profiles of Te, which are characteristic for the overflow cases. The initial (uncorrected) high-gain LP Te data indicate that they are systematically higher by about 300 K (~13 %) than their corresponding ISR measurements, but the correlations are again very strong (0.82-0.88). The regression model significantly improves the agreement between the two measurements by removing the systematic errors, and reducing $\tilde{\sigma}$s down to ~ 18-24 %, which is comparable to that for plasma frequencies. After testing the Ne-dependent and Ne-independent regression models, it was found that the Ne-dependence is statistically insignificant (at 5 % significance level) and therefore they are no longer considered here. The primary reason is related to the fact that the cases with overflows, which happen for large plasma densities when the LP is operating in the high-gain mode, are ignored. Below are new regression coefficients for the high-gain LP Te calibration and their comparison for similar models given in RD-1 supporting information.

Swarm A high-gain LP Te:

$T_{LP}^{adj} = 1.2844(\pm 0.0464) T_{LP} - 1083(\pm 127)$ (old: $T_{LP}^{adj} = 1.1925(\pm 0.0468) T_{LP} - 774(\pm 109)$)

Swarm B high-gain LP Te:

$T_{LP}^{adj} = 1.1626(\pm 0.0622) T_{LP} - 827(\pm 190)$ (old: $T_{LP}^{adj} = 1.1279(\pm 0.0214) T_{LP} - 642(\pm 124)$)

Swarm C high-gain LP Te:

$T_{LP}^{adj} = 1.2153(\pm 0.0410) T_{LP} - 916(\pm 111)$ (old: $T_{LP}^{adj} = 1.1025(\pm 0.0288) T_{LP} - 598(\pm 65)$).

Figure 3 is similar to Figure 2 but instead of the high-gain LP Te data it now compares the Swarm low-gain LP Te data to the ISR measurements. The low-gain LP also overestimate the electron temperature, however systematic errors are more than twice larger (~30 %) than those for high-gain LP. In addition, the correlation coefficients are lower for all three satellites and $\tilde{\sigma}$s are significantly larger. The difference between the two measurements is noticeably larger for certain large values of Te. Overall, the comparison shows that the Te values from the low-gain LP are less accurate, in agreement to the conclusion obtained in RD-1. Based on the obtained results these data should only be used when the high-gain LP Te data are not available or are not usable in the SITE estimate. In contrast to RD-1 results, a statistically significant part of the regression model is a simple offset correction, which even though removes systematic errors and reduces variability, $\tilde{\sigma}$ still remains at around ~36 %. The new (and old, Ne-independent) versions of correction models are:

Swarm A low-gain LP Te: $T_{LP}^{adj} = T_{LP} - 723(\pm 35)$ (old: $T_{LP}^{adj} = 1.4686(\pm 0.1058)T_{LP} - 2005(\pm 285)$)

Swarm B low-gain LP Te: $T_{LP}^{adj} = T_{LP} - 698(\pm 41)$ (old: $T_{LP}^{adj} = 1.2148(\pm 0.0604)T_{LP} - 1192(\pm 161)$)

Swarm C low-gain LP Te: $T_{LP}^{adj} = T_{LP} - 682(\pm 32)$ (old: $T_{LP}^{adj} = 1.4875(\pm 0.0849)T_{LP} - 1994(\pm 219)$).

The corrected Swarm LP Ne and Te data is expected to provide more reliable estimates of the ion temperature by SITE.

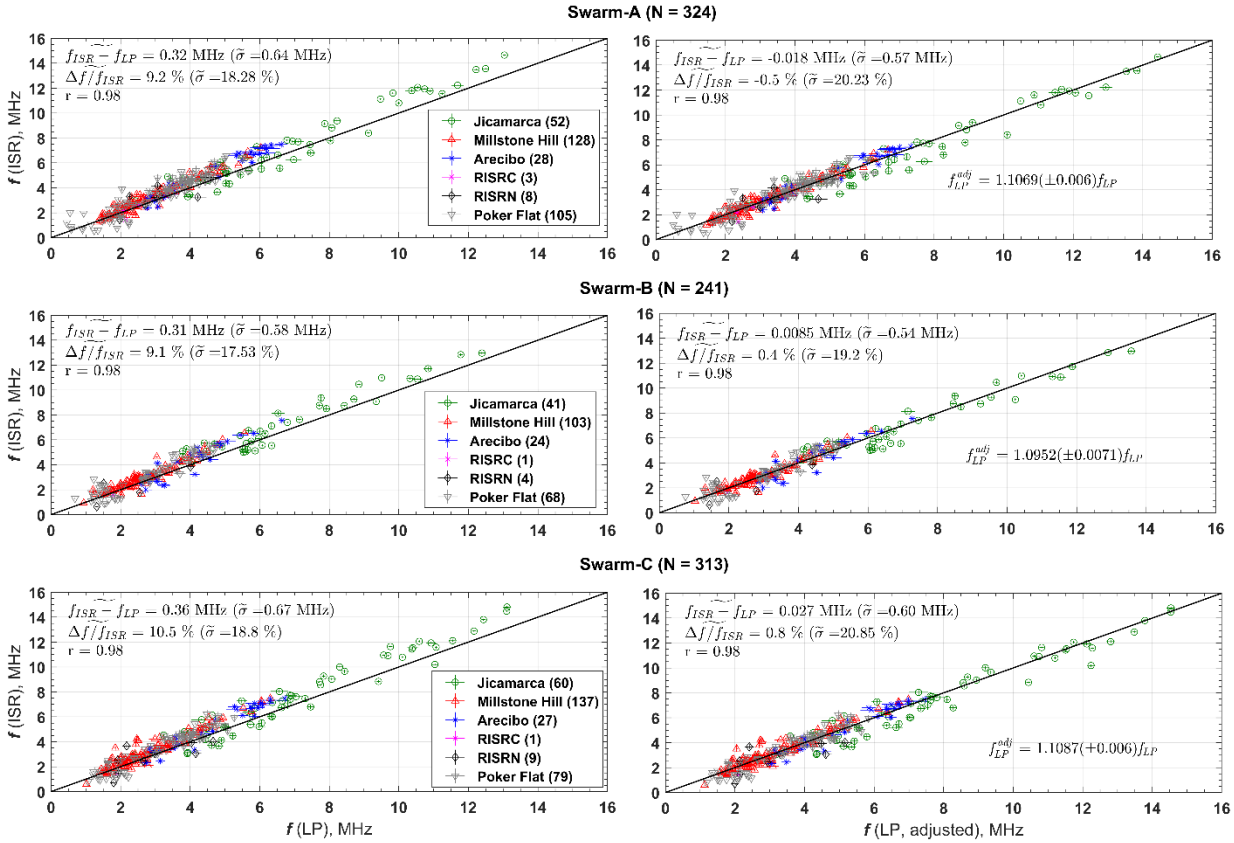

Figure 1: Comparison of (left) initial and (right) calibrated Swarm LP plasma frequencies to corresponding ISR measurements. Shown also are medians of absolute and relative differences with corresponding (scaled) median absolute deviations (equivalent to 1-sigma), correlation coefficients, and a regression

model used to adjust the data. The black lines are identity lines. The numbers in the brackets are standard errors of the regression coefficients.

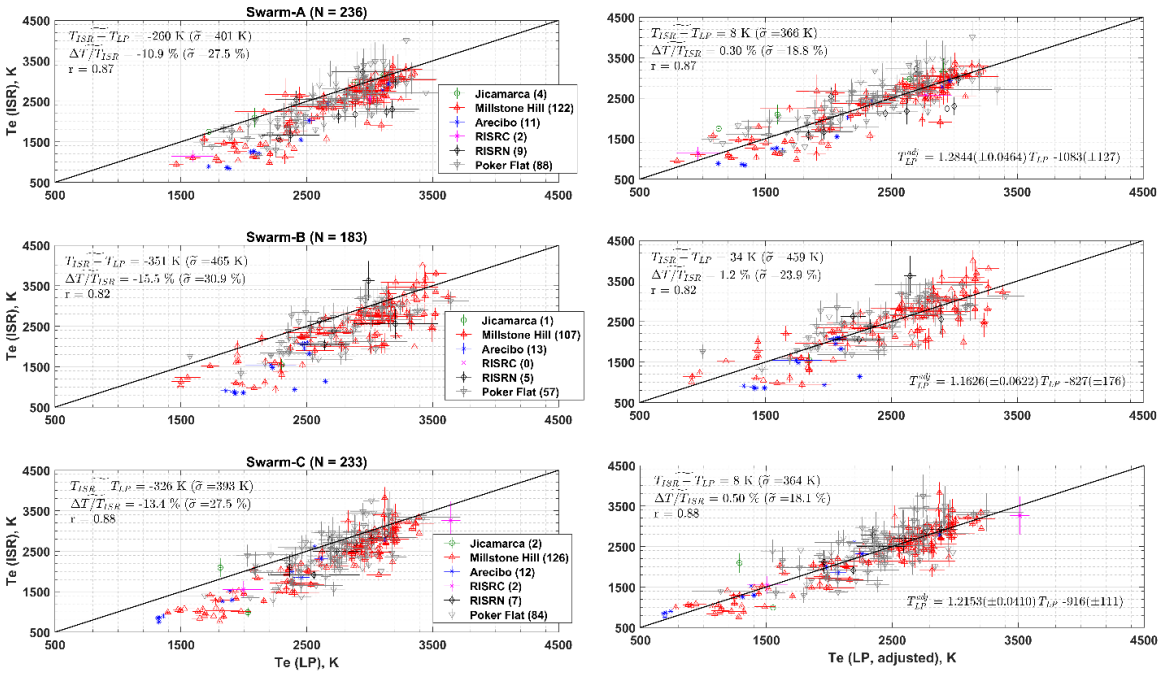

Figure 2: Same as Figure 1 but for high-gain LP Te.

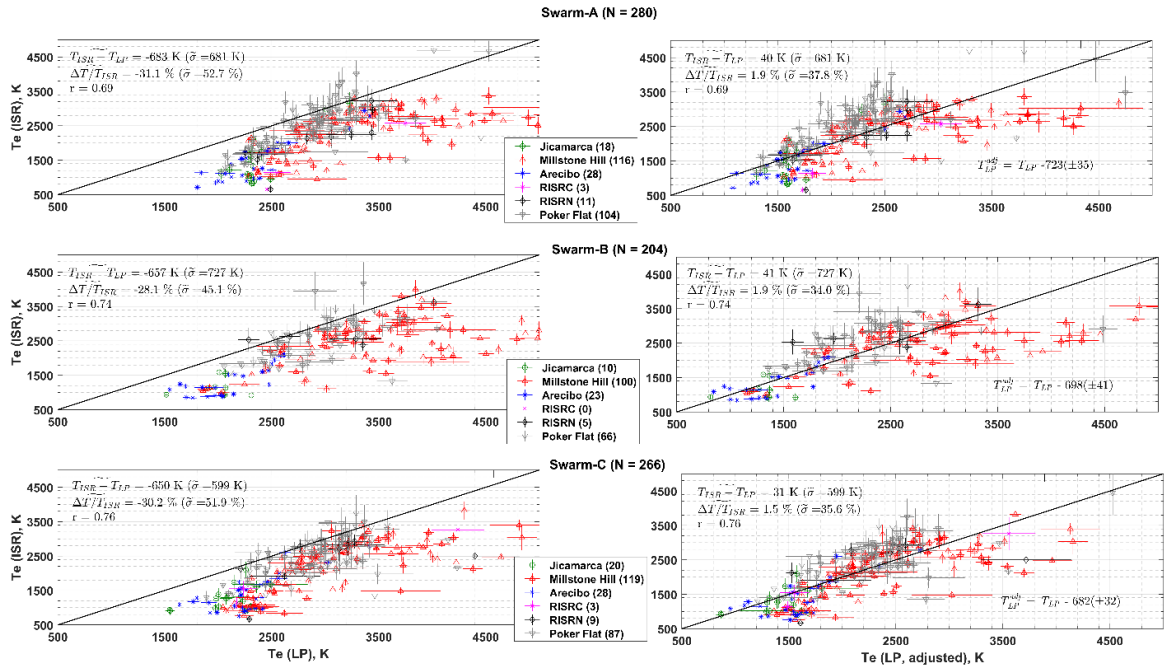

Figure 3: Same as Figure 1 but for low-gain LP Te.

3.2 Swarm TII drifts

In addition to the Swarm LP data, the SITE model uses plasma drift estimates in the high-latitude ionosphere to specify ion frictional heating in the ion heat balance equation [RD-4]. Independent estimates of

these drifts are provided by Swarm TII measurements [RD-5] and Weimer 2005 (hereafter W05) empirical convection electric field model (W05) [RD-6], giving two different estimates of the ion temperature at high latitudes. Consequently, it is important to evaluate validity of the TII ion drift measurements and their consistency with the W05 model. In this report a validity study was conducted for newly recalibrated TII ion drifts (TCT version 0302), and the focus was on all three components of the drifts, which are horizontal cross-track and along-track, and vertical cross-track drifts. The validity of the TII horizontal cross-track flows has been evaluated in RD-3, which used version 0101 of the data between Nov/2015-Jul/2017. The current release (version 0302) however spans the period between Dec/2013 and Sep/2020, and the processing and calibration algorithm has been updated [RD-5], making their reassessment essential.

The evaluation of the Swarm TII drifts was conducted by analysing median drift patterns in the high latitudes and by their comparison with Weimer 2005 model estimates, similar to RD-3. The high-latitude drifts are known to be organized by magnetic latitude and local time, and they show clear dependence on interplanetary magnetic field (IMF) parameters [RD-3, RD-6]. Therefore, the TII horizontal drifts were first projected to magnetic east and north directions and then the median values for a given MLAT and MLT bin were calculated for four different orientations of IMF: By>0, Bz<0; By<0, Bz<0; By>0, Bz>0; and By>0, Bz<0. Analysis was done for northern and southern hemispheres (NH and SH) and for each Swarm satellite separately. For the sake of computing efficiency, one of every eight Swarm TII observations were used (i.e., every 4 seconds). For each Swarm observation the W05 model was run using observed IMF conditions and solar wind conditions (but without the AL index dependence). The horizontal cross-track and along-track drifts were calculated and then were binned similar to the Swarm data to create the model-based median ion drift distribution (maps). In this data evaluation a quality flag=1 was used for Swarm A and B cross-track drifts. The along track and vertical drifts and all Swarm C drifts have only quality flag=0, therefore in the subsequent analysis for Swarm A and B along-track and vertical drifts used were only those which have corresponding cross-tack flag=1, but for Swarm C all available data were used.

3.2.1 Horizontal Cross-track drifts

The MLAT-MLT maps of the northern hemisphere high-latitude zonal median ion drifts obtained from the Swarm A horizontal cross-track ion flow measurements for four different orientations of the IMF are given in Figure 4. The positive values are for the magnetic eastward direction. Left panels are for Swarm TII and right panels are for their corresponding W05 estimates. The TII data show the ion drifts that are well organized by MLAT and MLT with very clear reversal boundaries. The median flow magnitudes are largest near 70° MLAT and can reach up to ~750 m/s. There is a clear IMF By-dependent asymmetry (compare 1st to 2nd and 3rd to 4th panel in Figure 4). In addition, the flows are stronger, and the convection patterns are expanded towards lower latitudes when IMF Bz is southward (i.e. Bz<0) (compare 1st to 4th and 2nd to 3rd panel in Figure 4). Figure 4 also indicates close correspondence between the Swarm TII and W05 model data. The two estimates agree in magnitude, in their response to IMF orientation changes, and location of flow reversal boundaries. These findings are consistent with those reported in RD-3, however Swarm-based maps display less gaps, are smoother, and appear to agree better with the model. Furthermore, a quantitative evaluation based on practically identical version 0301 data between 2013-2018 shows improved correlation (0.87-0.91), reduced RMSD (81-108 m/s), and reduced $\tilde{\sigma}$ (68-93 m/s) when median drifts from Swarm TII and W05 are compared.

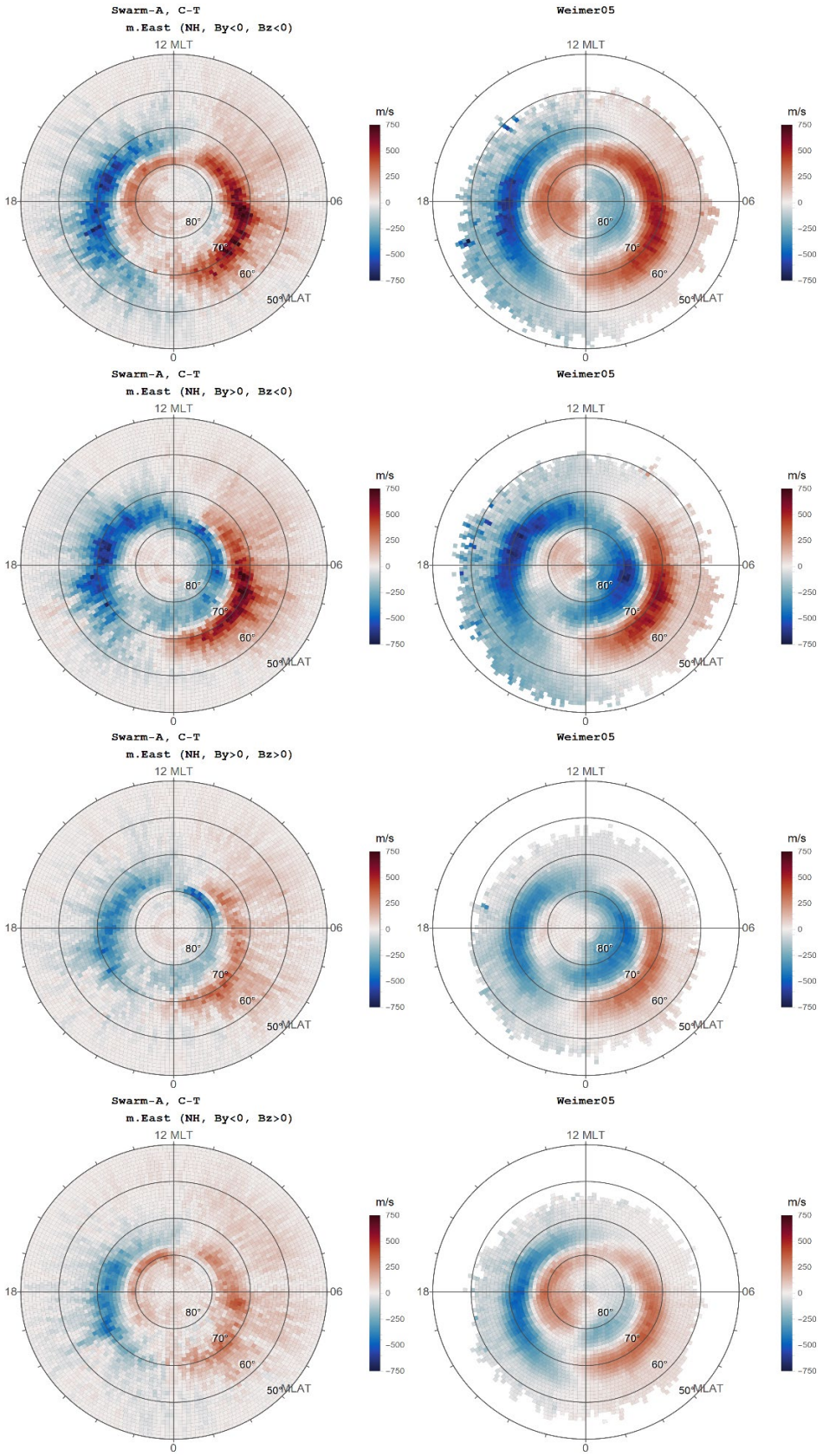

Figure 4: Magnetic eastward projections of Swarm A horizontal cross-track drifts in the northern hemisphere for different IMF orientations.

In addition, it shows that the Swarm A TII cross-track magnitudes are about 10 % smaller overall than Weimer 2005 drift magnitudes, which is a noticeable improvement relative to the earlier version of the data, which showed are marked overestimation of drift magnitudes relative to W05.

Figure 5 compares Swarm A, B, and C median magnetic eastward drifts from cross-track measurements in the northern hemisphere for the IMF By>0, Bz<0 conditions. The results from three satellite are generally consistent with each other and with W05 model results, both quantitatively and qualitatively. The largest difference however can be noticed near the pole. The Swarm C data are noisier, partially because they are limited in amount, and they also are relatively smaller in magnitude than those from W05.

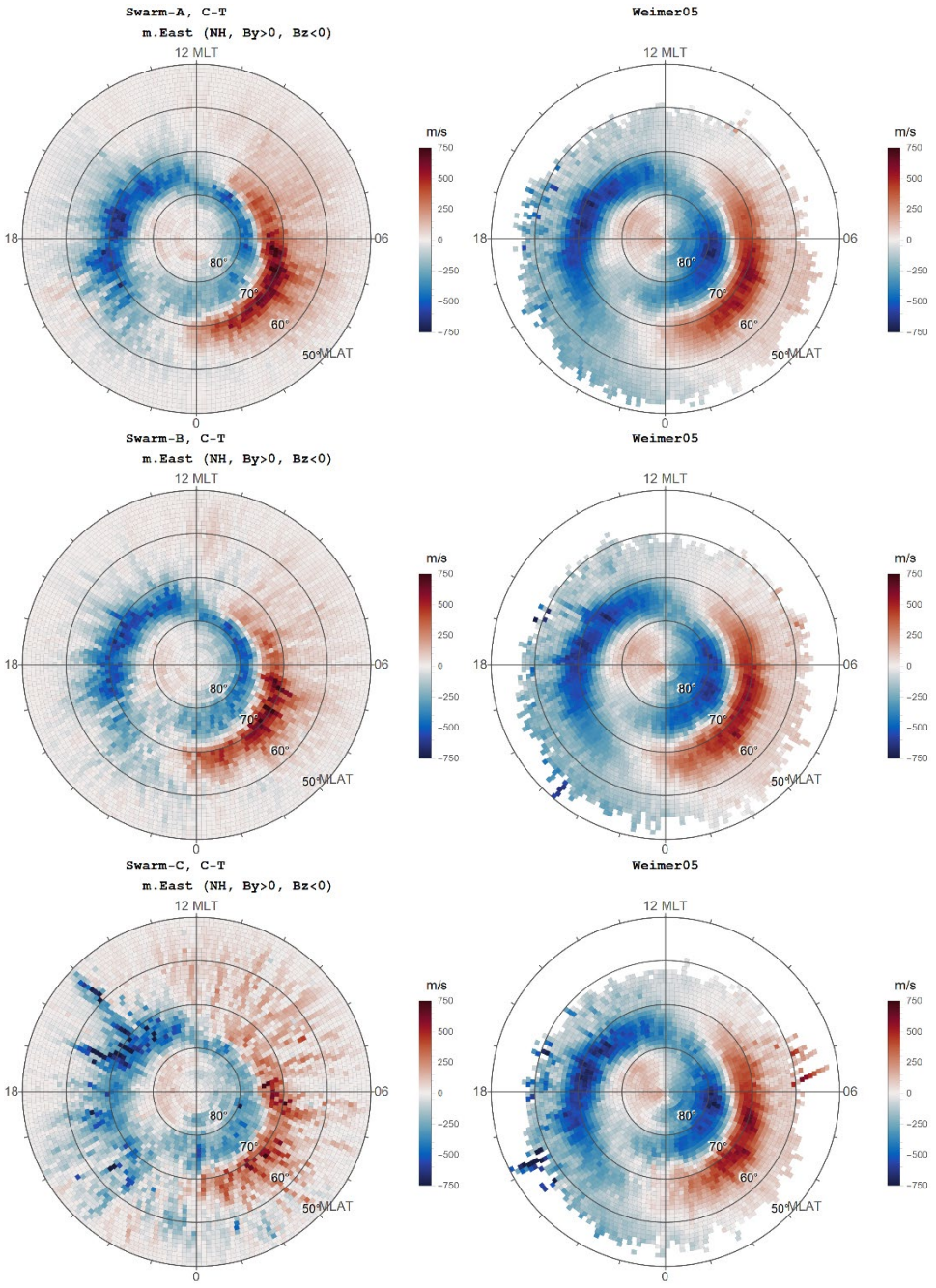

Figure 5: Magnetic eastward projections of Swarm A, B, and C horizontal cross-track drifts in the northern hemisphere for IMF By>0, Bz<0.

Figure 6 is similar to Figure 5 but it is for the southern hemisphere. It again compares results from three satellites to each other and with their corresponding W05 estimates. The results appear consistent, indicating a valid TII cross-track data. The gross features of the eastward components of the cross-track drifts in the SH share some similarities with those in the NH, however there are differences, particularly in overall flow magnitudes and in drift variations near the poles. Note, it is known that for a given By direction the NH and SH electric potentials appear as 'mirror images'. This effect is noticeable from Figure 5 and 6.

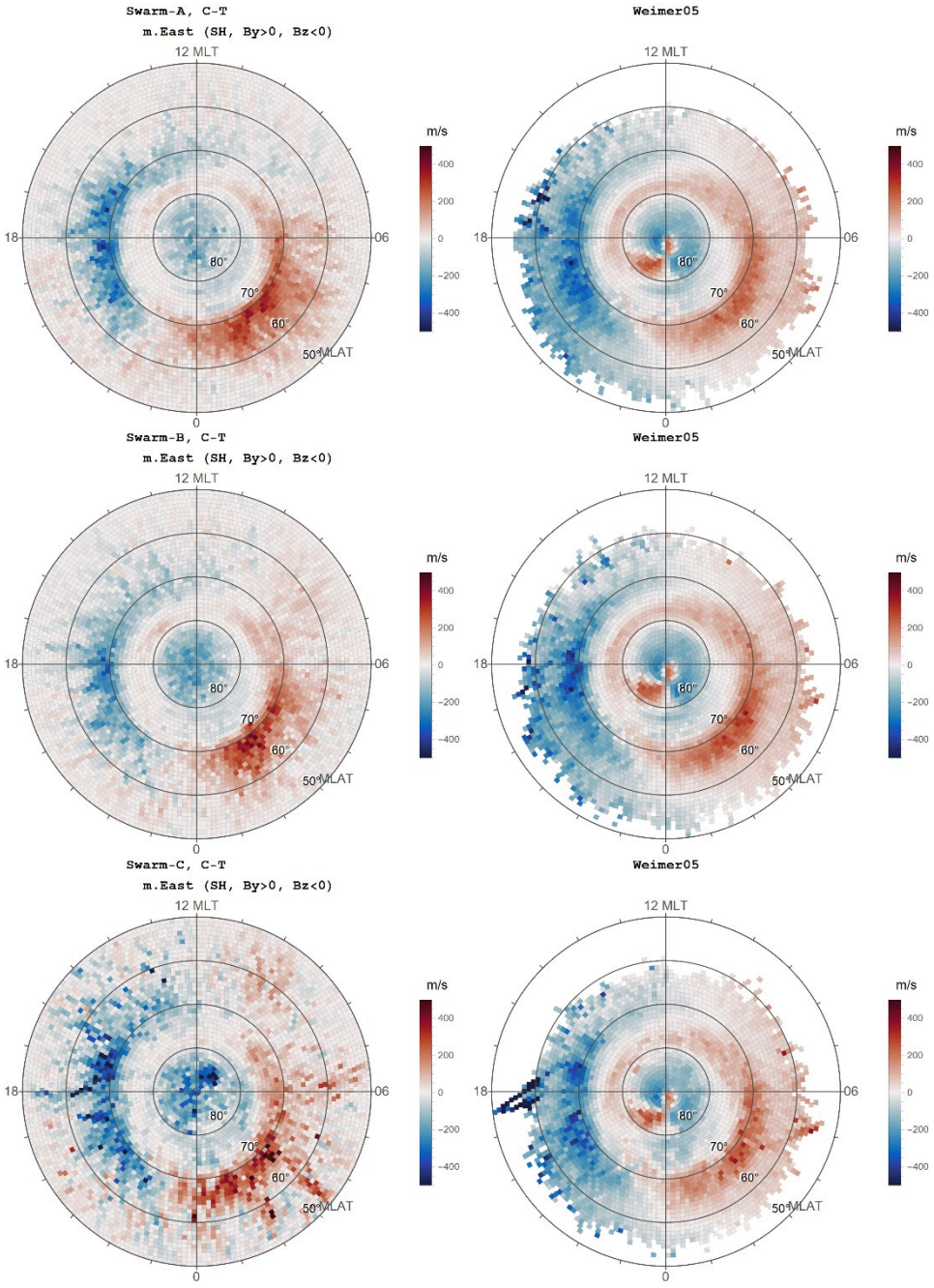

Figure 6: Same as Figure 5 but for the southern hemisphere.

Overall, these results demonstrate the improved quality of new 0302 version of the TII cross track horizontal drifts and their validity for the SITE to be included in the estimation of the ion temperature for all three satellites, thus including Swarm C.

3.2.2 Horizontal Along-track drifts

The Swarm along-track drifts are obtained separately from the two (horizontal and vertical) on-board TII instruments. These drifts are known to be more sensitive to instrument noise and external factors and currently are not validated. In addition, there are several assumptions made to estimate these flows, which have potential to limit the accuracy of these data [RD-5]. Most notably, the ion composition and satellite floating potential are both assumed to be constant within a given pass through a polar region. Nevertheless, it is important to assess the validity of this data, for which the procedure similar to that for cross-track flows are followed.

Figure 7 presents maps of magnetic eastward projections calculate from the median along-track drifts in the southern hemisphere for IMF By>0, Bz<0 conditions from both horizontal (H) and vertical (V) sensors and from W05. The TII drifts from both sensors show clear MLAT and MLT pattern, which are very close to each other. There are some similarities with W05 results at lower latitudes, but at higher latitudes and near the pole there are significant differences. The Swarm along-track drifts appear not to be able capture the flow reversals that are seen in the W05 data around dawn period. The case for different orientation of the IMF (not shown) also shows similar discrepancies but in the same time indicates the TII along-track flows responds to the changing IMF conditions properly.

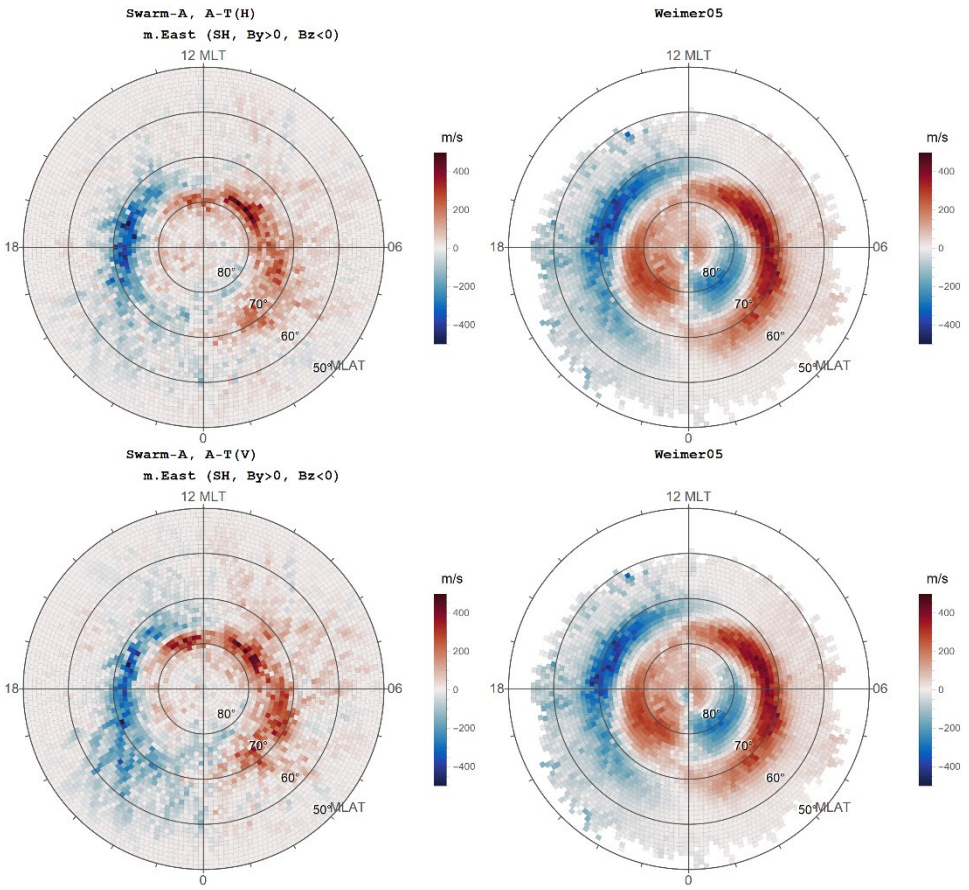

Figure 7: Magnetic eastward projections of Swarm A horizontal along-track drifts in the southern hemisphere for IMF By>0, Bz<0 condition.

Figure 8 and 9 are similar to Figure 7 but for Swarm B and C. Swarm B drifts from horizontal and vertical TIIs are again close to each other but the discrepancies between them and the W05 model are evident. Swarm C shows even more discrepancies and between the model results and between the two sensors.

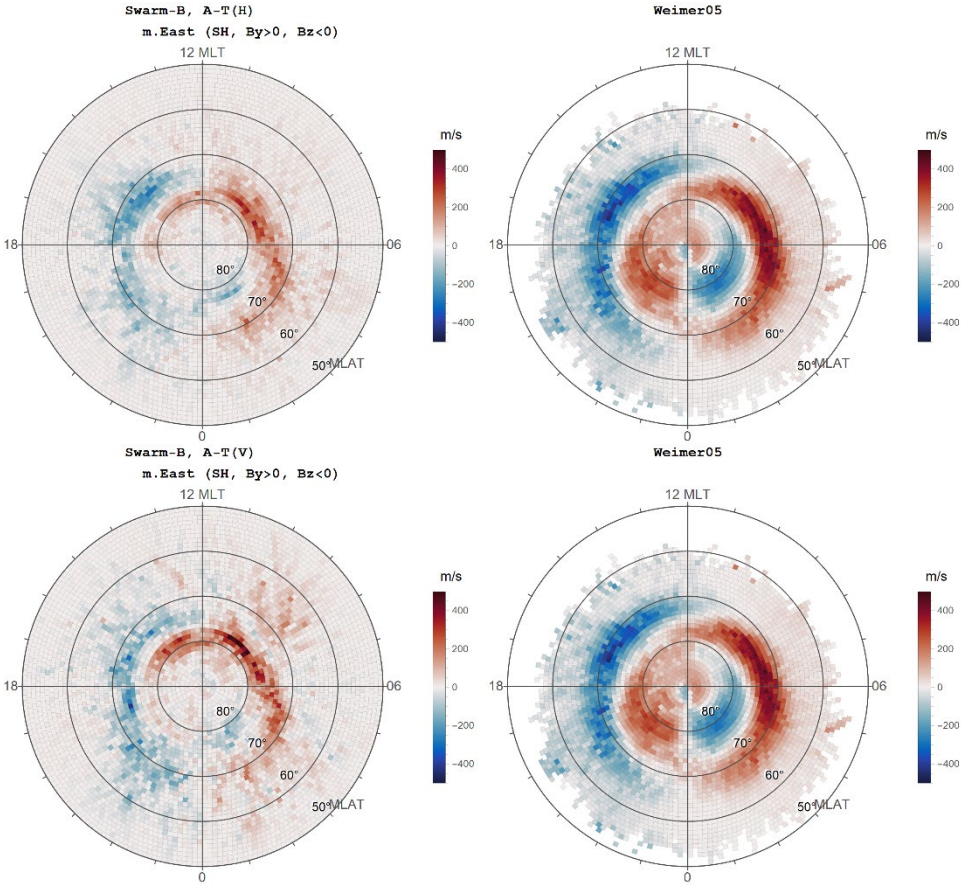

Figure 8: Same as Figure 7 but for Swarm B.

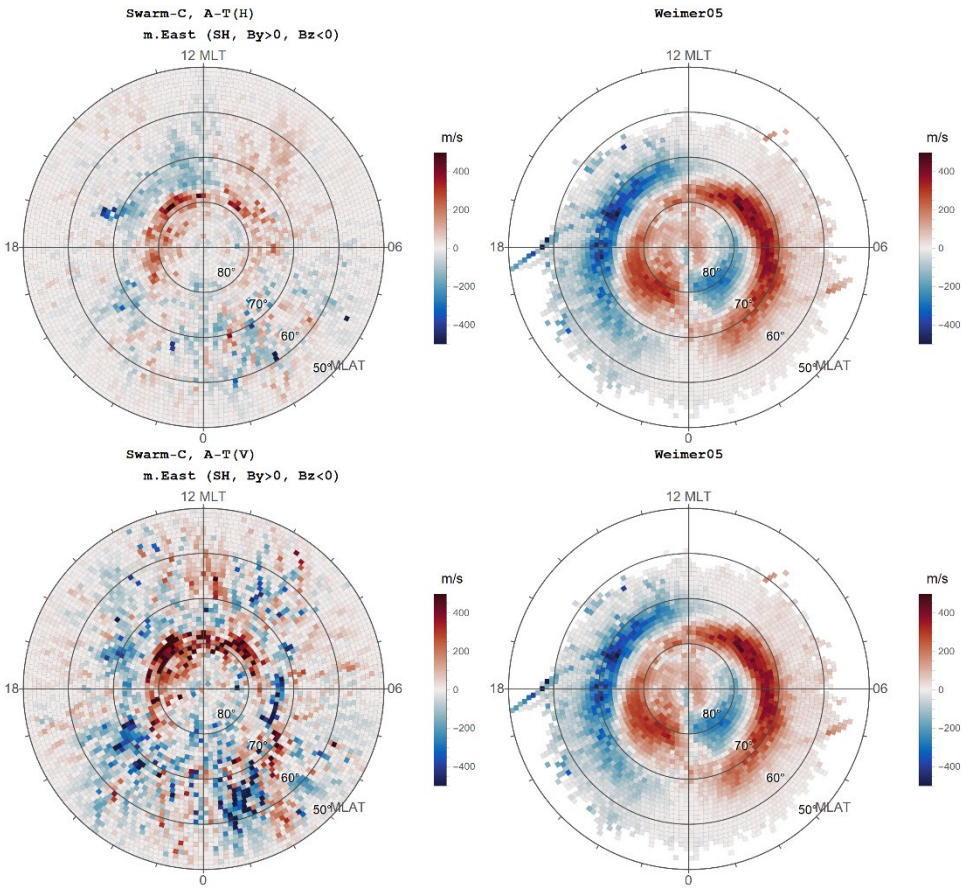

Figure 9: Same as Figure 7 but for Swarm C.

To further evaluate the along-track drift data, Figure 10 shows results for the NH but for the median magnetic northward projections of the along-track flows which, different from the SH, are expected to be relatively stronger than the eastward projections. The results of two sensors do not appear to be as close to each other as they were for the SH (Figure 7), and more importantly, they are significantly different from the W05 drifts, which clearly show the existence of the anti-sunward cross-polar cap flow. These discrepancies also appear in Swarm B and C along-track TII data when similar maps are examined, and for other IMF orientations.

It is known that the DE-2 satellite measurements used to construct the W05 model had fewer measurement in the southern hemisphere, and therefore the observations from both hemispheres were mixed, accompanied by a reversal of signs of both the IMF By and the dipole tilt angle [RD-6]. This may result in the poorer accuracy of the W05 model in the southern hemisphere, and some discrepancies between it and measurements are expected. However, the fact that the cross-track measurements agree better in the southern hemisphere indicates that the likely real large-scale features in the SH ion convection cannot be captured by the Swarm along-track drift measurements. In addition, the along-track measurements in the northern hemisphere indicates that they do not capture the gross features of the ion convection and measurements from the two sensors are different. In view of these facts, the use of Swarm along-track TII drifts in SITE to estimate the high-latitude frictional heating is not advisable until better estimates of these flows are available. Note that the work to improve these drifts is ongoing.

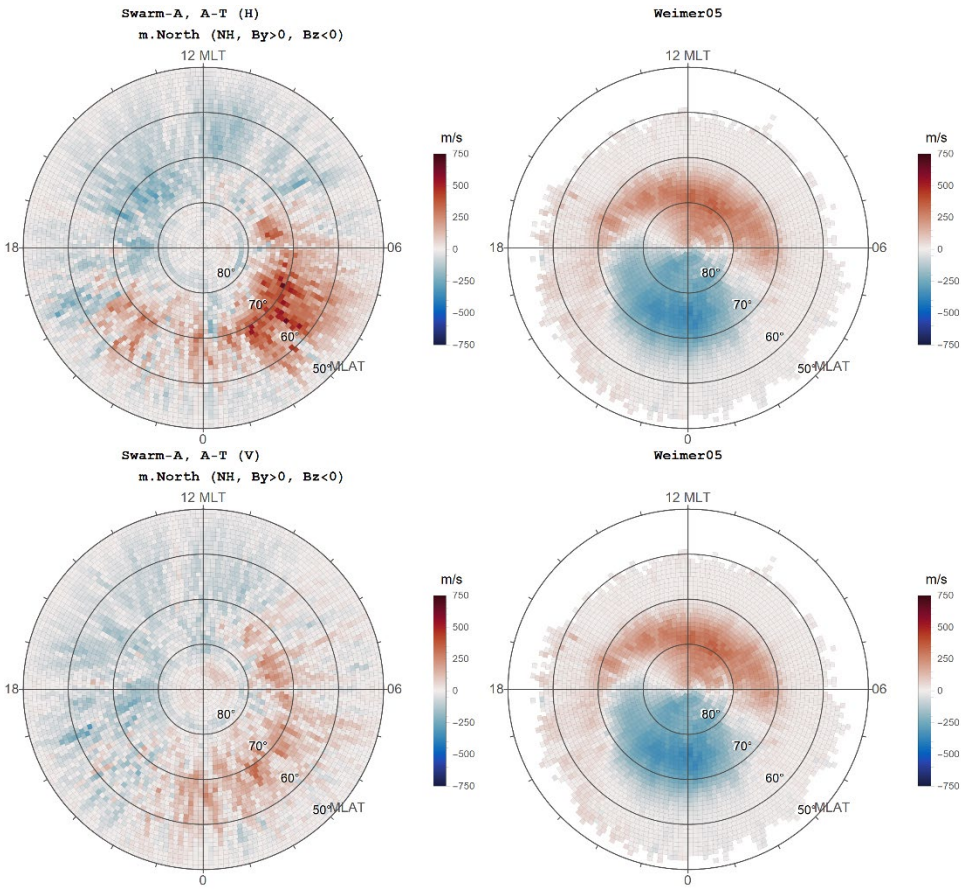

Figure 10: Magnetic northward projections of Swarm A horizontal along-track drifts in the northern hemisphere for IMF By>0, Bz<0 condition.

3.2.3 Vertical Cross-track drifts

The vertical (radial) ion drift in the high-latitude ionosphere results from various processes and some of dominant ones are not related to the convection electric field [RD-7]. Therefore, the use of W05 model is not relevant to study the validity of this drift component. Nevertheless, there are well known features that are characteristic for the ion upflow, such as upward plasma flow equatorward of polar cap, cusp ion upflow near noon, and return downward flow over the polar cap. Their pattern is also dependent on season, geomagnetic conditions (Kp) and the IMF orientation, displaying asymmetry based on the IMF By, and flow speed modulation by the IMF Bz. To examine these patterns MLAT-MLT maps were constructed of the vertical ion drifts for the different IMF orientations. Results for Swarm A in the northern and southern hemispheres for the southward IMF and opposite IMF By are given in Figure 11 (note a colour-scale difference between these and horizontal drifts). Top panels are for the NH and bottom panels for the SH. Left and right panels have opposite By sign and positive values indicate downward flows. The vertical drifts show a clear tendency of being downward over the polar cap. There is also an indication of a By-dependent asymmetry in this downward flows, and northern and southern hemisphere results exhibit a 'mirror symmetry'. In addition, equatorward of the polar cap there are bands of the upward flow. These all agree with the expectations. However, it is also clear that the there is a significant variability at lower altitudes, likely indicating a signal contamination, large measurement noise or insufficient offset correction.

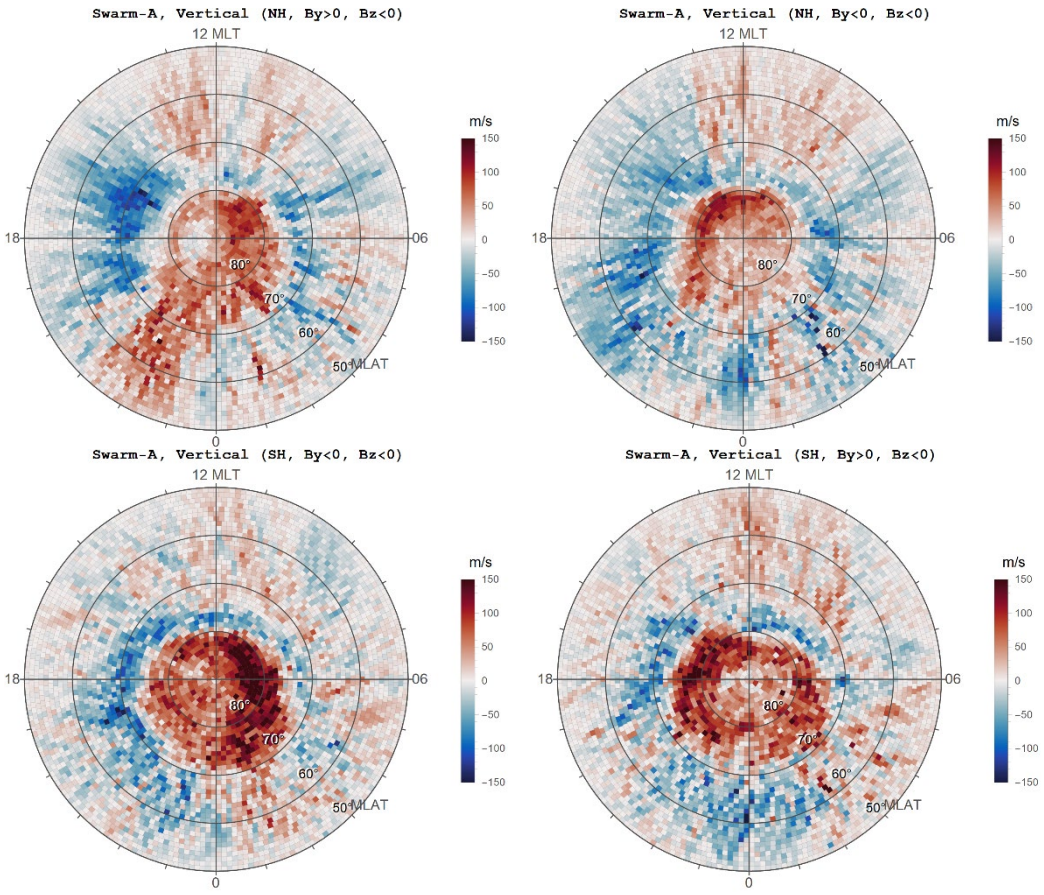

Figure 11: Swarm A vertical (radial) ion drift maps in the (top) northern and (bottom) southern hemisphere for the IMF Bz<0 and different By orientations

Swarm B shows comparable or occasionally noisier vertical drift data, but the main features seen in Swarm A data are also identifiable. Swarm C vertical ion drift data indicates significantly larger flow magnitudes and noise. Given the current findings it is apparent that the Swarm TII vertical cross-track drifts require further processing and calibration, therefore they should be omitted from the SITE.

3.3 SITE ion temperatures

3.3.1 Overview

The primary parameter provided by SITE data products is estimated 2Hz ion temperature (Ti) along the orbits of three Swarm satellites in the topside ionosphere. The estimation is based on the ion heat balance equation, and at high magnetic latitudes (poleward of 60°MLAT) the effect of ion frictional heating is also included. For the ion frictional heating estimation, the ion drift velocity is calculated using both Swarm TII and Weimer 2005 empirical convection electric field model [RD-12, RD-4]. Consequently, there are two different estimates of ion temperature at high latitudes. Their values are identical at low and middle latitudes where no frictional heating is specified. Current version of the SITE includes the all components of the TII-measured drifts except for Swarm C. This is planned to be updated based on the results of this report, indicating that the only horizontal cross-track drifts are reliable in the current 0302 version of the TII data, including those for Swarm C.

The corrections in Swarm LP Ne and Te outlined in this report were used to remove their systematic errors that bring their values closer to independent measurements made by ISRs. In the Ti estimation the values of Te are taken from Swarm high-gain LP whenever possible, however if the high-gain LP Te is not available or is not usable, then low-gain LP measurements are used if feasible. The required neutral atmospheric parameters are calculated using empirical models, NRLMSISE-00 [RD-8] and HWM14 [RD-9].

Figure 12 shows examples of latitudinal profiles of estimated ion temperature (red) for Swarm A on 25 July 2014. Shown also are the corrected profiles of Swarm LP electron temperature (purple) and neutral temperature (Tn) (green) from NRLMSISE-00. The profiles are divided between geographic south and north poles, and the parameters on each panel are UT (accurate to within 1 sec), local solar time (LST) and geodetic longitude for the moment the satellite was closest to the geographic equator. The high latitude frictional heating in this example is calculated using the Swarm TII data.

From Figure 12 it can be seen that at low and middle latitudes the ion temperature is between those of electrons and neutrals and displays reasonable latitudinal variation. It is expected for the ion temperature to have intermediate values between Tn and Te at Swarm altitudes, since the ions are primarily heated by electrons and cooled by neutrals. The heating and cooling rates also depend on densities of both electrons and neutral species. At high latitudes there is a noticeable enhancement of the ion temperature due to both hot electrons and ion frictional heating.

The low latitude daytime ion temperature jumps (right panels in Figure 12) arise because of the switch between high-gain and low-gain LP Te in the estimation process. The unavailability of high-gain LP Te can occur because of the so-called LP overflows [RD-2] but may also happen if the electron temperature is overcorrected and drops below the neutral temperatures. In such cases the ion temperature cannot be determined from the high-gain LP Te. The use of low-gain LP Te is reserved for such cases. It should be noted that in the high-gain LP Te validation, very few ISR measurements from Jicamarca ISR contributed to the

regression model (Figure 2). More equatorial electron temperature data should enable further adjustment to the Te correction model.

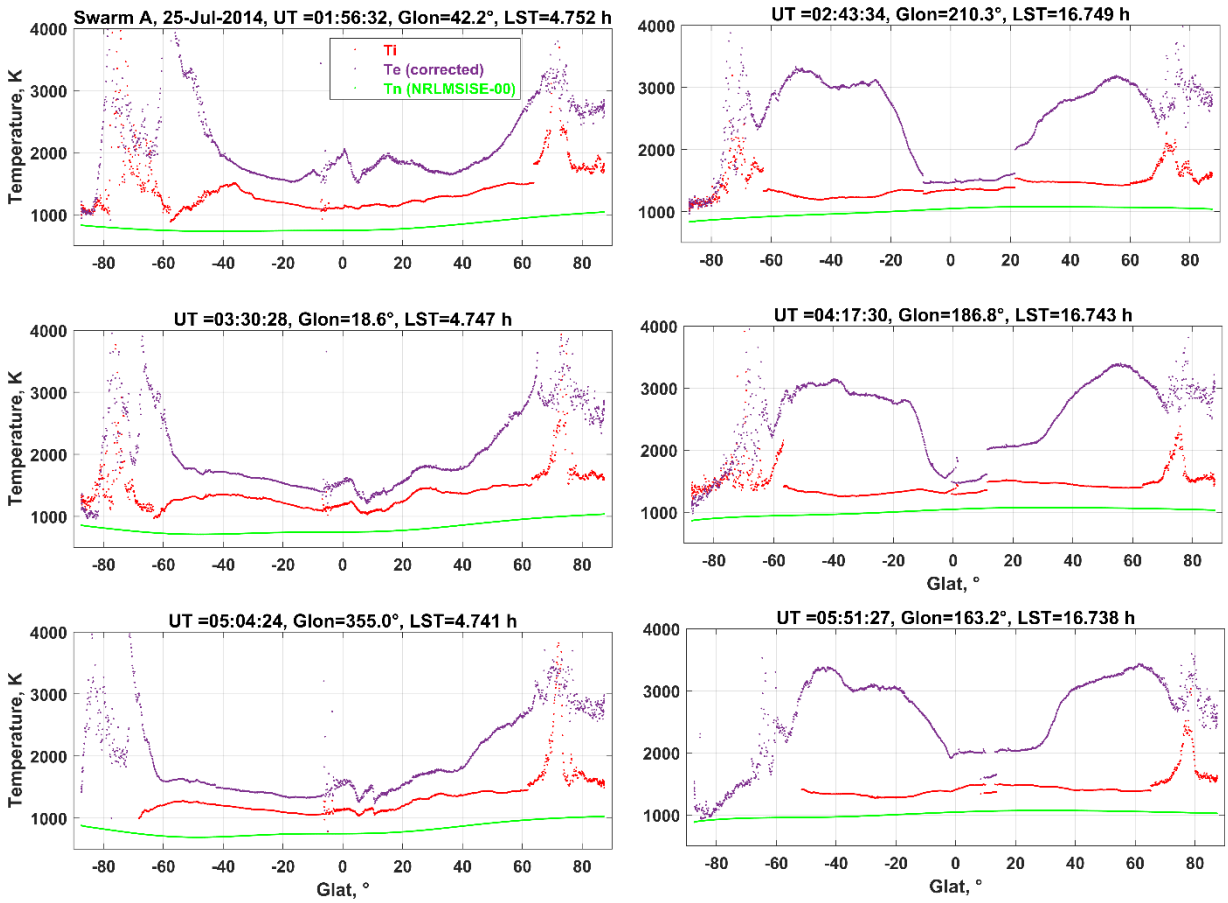

Figure 12: Latitudinal profiles of estimated (TII-based) ion temperature (red), corrected Swarm LP electron temperature (purple), and NRLMSISE-00 neutral temperature (green) in the ionosphere along the orbits of Swarm A satellite on July-25, 2014. Time and longitude on each panel is at the crossing of geographic equator.

Figure 13 presents two estimates of the ion temperature (TII-based and W05-based) which differ only at high latitudes. The TII-based estimates tend to be higher, however the two temperatures correlate well and both show similar features of the temperature. Note that the TII-based estimates shown here include Swarm-along-track and vertical drifts, which when erroneous could cause large overestimation of ion temperature. The next revision of the SITE Ti processing will omit these drift components as discussed above.

Also noticeable in Figure 13 are discontinuities at transitions from mid- to high-latitude. These arise from artificially setting the frictional heating boundary at 60° MLAT in SITE. Both TII and W05 drifts are usually available equatorward of this boundary where they show smaller drift magnitudes. Setting lower boundary at, for example 50°, should eliminate such high-latitude jumps and provide smoother transitions.

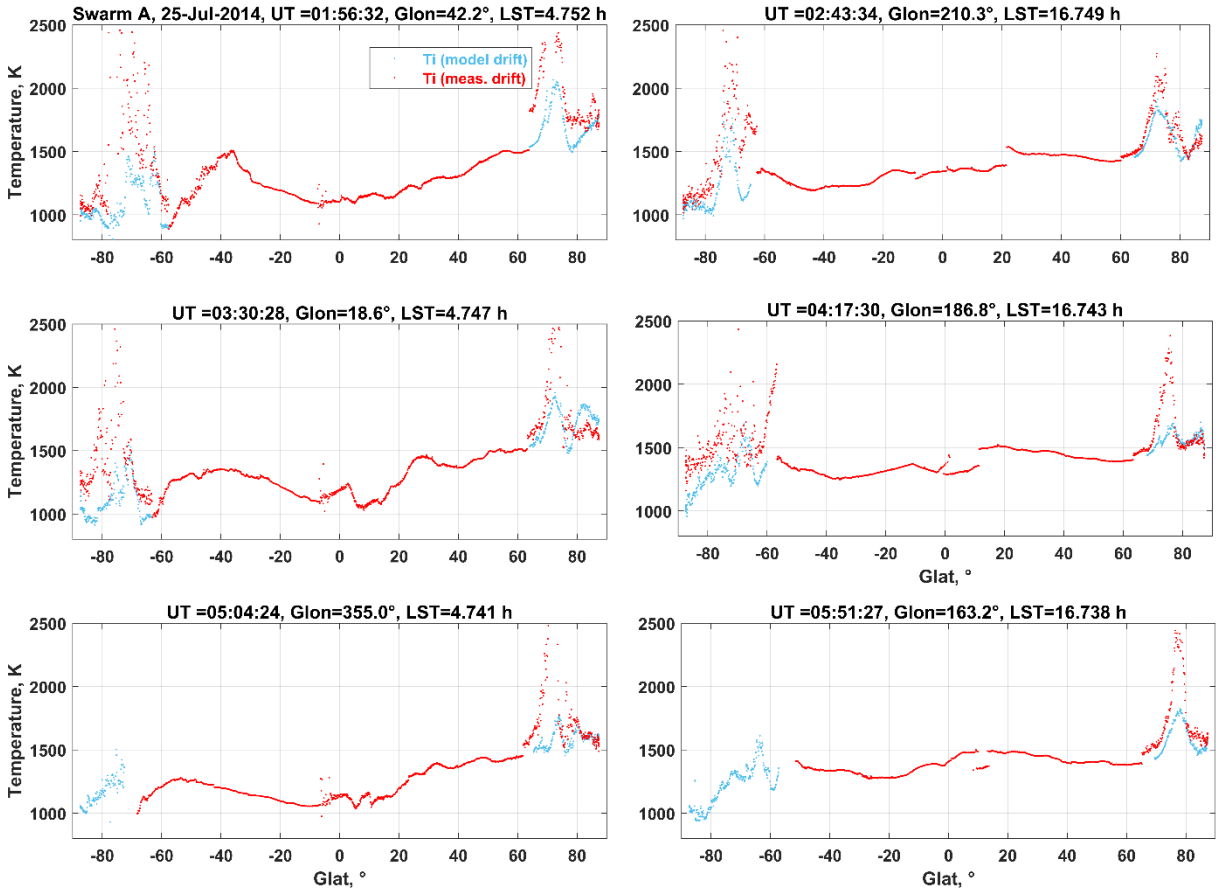

Figure 13: Latitudinal profiles of estimated ion temperatures in the ionosphere along the orbits of Swarm A satellite on July-25, 2014. Red colour corresponds to the ion temperature for which the estimation used Swarm TII ion drifts at high latitudes, and light blue colour corresponds to the temperature when Weimer 2005 drifts are used instead of TII drifts. The two temperatures are identical at low and middle latitudes. Time and longitude on each panel is at the crossing of geographic equator.

3.3.2 Validation against ISRs measurements

The approach used to validate the estimated ion temperatures is similar to those for Swarm LP Ne and Te and was described in Section 3.1. The validation period covers only about 3.5 years (Dec/2013 – May/2017), or half of the Swarm mission, and is based on the currently available preliminary dataset (DL-02).

Figure 14 shows typical examples of the ISR measurements of the ion temperature at Millstone Hill, Arecibo, and Poker Flat, during the conjunctions with the Swarm A satellite. The SITE Ti values, averaged within a pass are indicated in blue, and the interpolated ISR measurements at the altitude of Swarm are shown in green. Parameters on the top show the distance between the Swarm and ISR measurement at Swarm altitude, relative error of the ISR measurement, date, local solar time, ISR Madrigal database specific datatype code (kindat), and the Ap index. These examples demonstrate that the SITE ion temperatures are close to the ISR data.

Next, all available coincident measurements and estimates were collected and compared. The separate comparisons are done for cases with and without the use of low-gain LP Te, and also for the TII-based and W05-based estimates.

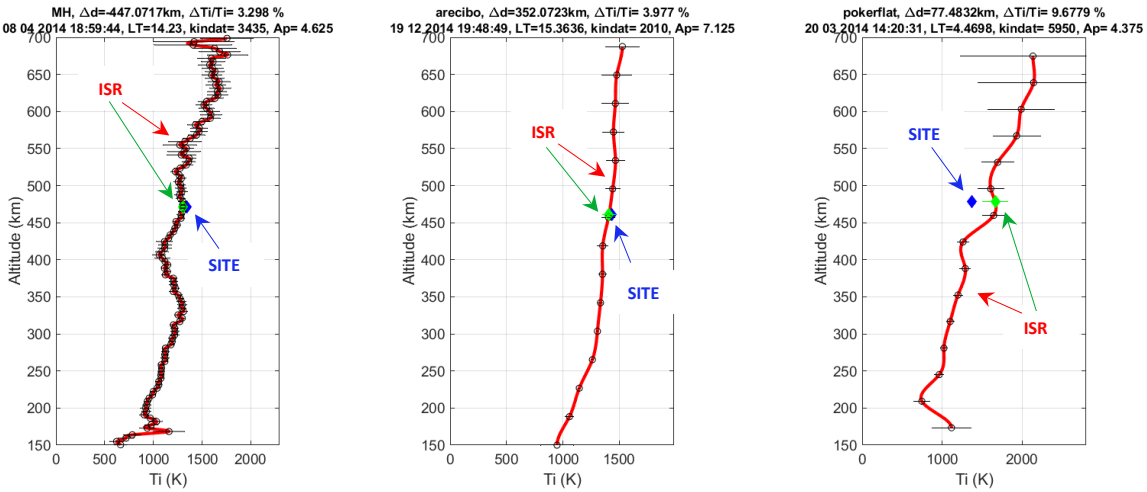

Figure 14: Examples of coincident ISR profiles of ion temperature (red), their interpolated values at Swarm altitude (green), and SITE ion temperatures (blue).

Figure 15 presents comparisons for the TII-based ion drifts for all three satellites. Note that the TII data contributed only to high latitude estimates at RISR-C, RISR-N and Poker Flat ISR sites. Left panels are for all available Ti data and right panels are for cases when only high-gain LP Te were used. The total number of cases varies between 77 and 147. The number of measurements from each ISR is indicated on the corresponding panel.

The comparison shows that the SITE ion temperatures agree well with the ISR data. They are within ~8 – 18 % (1-sigma) to the ISR measurements and show strong correlation (0.63-0.87) indicating a reliability of the SITE method. The statistical parameters seen in Figure 15 are well within the limits predicted by the model data when the accuracy of the method was evaluated [RD-4]. The results are also comparable to those seen for initial Swarm LP Ne and Te data. Though not excessive, there is an obvious overestimation of temperature by SITE of about 11-13 % (~121-157 K) for all satellites. The correlation coefficients are smaller for Swarm B, and larger for Swarm C, but the latter does not include the high-latitude owing to the omission the Swarm C TII drifts. The correlation is better for cases when only high-gain LP Te data are considered, which is expected given the higher accuracy of these measurements. The relatively small number of high latitude measurements is insufficient to rigorously evaluate the high-latitude ion temperatures. The general tendency seen at middle and low latitudes does appear to apply to the high-latitude data. Inclusion of more data, which is planned, should provide a better indication of the ion temperature validity at high-latitudes.

One of the primary candidates for explaining the systematic error in SITE data is a possible error in the O-O^+ collision frequency. This parameter is known two have an uncertainty of about a factor of 2 [RD-10]. The SITE processor [RD-12] uses the ion-neutral collision frequencies given by RD-11. Analysis of the dependence of the estimated ion temperature on the O-O^+ charge exchange collision frequency and use of its most accurate form in the energy transfer in is needed. Generally, larger collision frequency should provide more cooling of ions via neutrals, and thus reduce the ion temperatures. Furthermore, based on theoretical validations [RD-4] the model used for SITE is more likely to underestimate temperature. Errors in the neutral atmospheric parameters are not expected to be able to explain systematic errors of ~140 K.

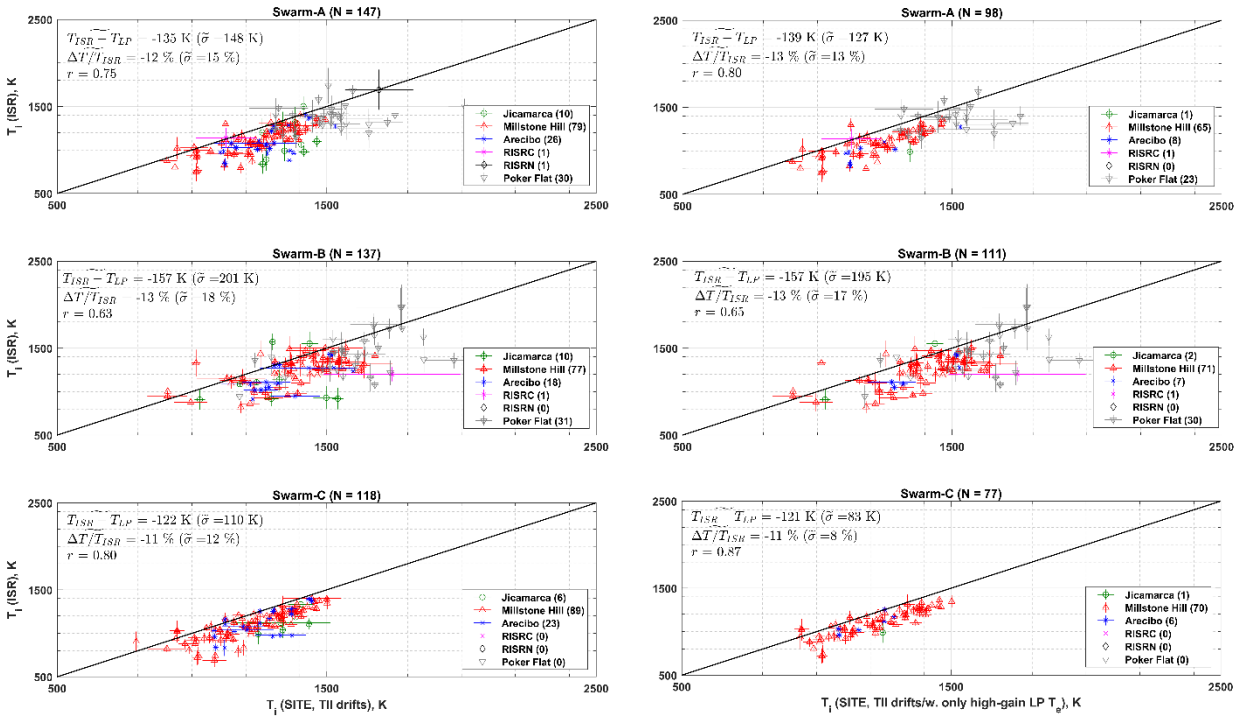

Figure 15: Comparison of SITE ion temperature estimates to their corresponding coincident ISR measurements for Swarm A. Left panels correspond to all available data and the right panels to only those cases when the Swarm high-gain LP Te data were used. Each panel also shows medians of absolute and relative differences, their (scaled) median absolute deviations (equivalent to 1-sigma) and correlation coefficients. The black lines are identity lines.

Finally, Figure 16 compares the ISR and SITE ion temperatures for cases when the high-latitude drifts are taken from W05 instead of the TII data. Results for Swarm A and C display only small changes in the statistical parameters, and there are some improvements in the correlation for Swarm B, but overall picture remains similar to that in Figure 15. Exclusion of TII along-track and vertical drifts from SITE and extending the validation period for the full mission is expected to provide more accurate pictures.

Overall, the comparisons shown here indicate very good agreement between the SITE and ISR data, and together with the validity study of Swarm LP and TII data provides an opportunity for further improvements of the SITE products.

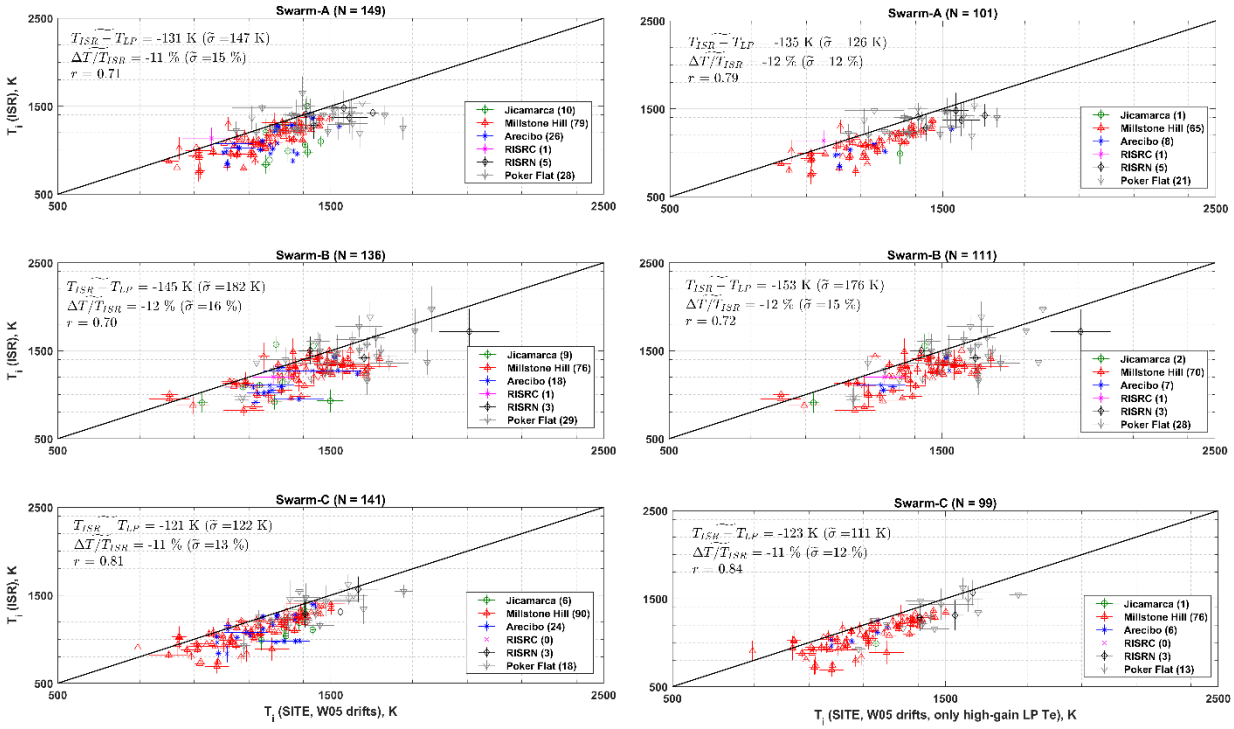

Figure 16: Comparison of (left) initial and (right) calibrated Swarm LP plasma frequencies to corresponding ISR measurements.